Study on the influence of vegetation change on runoff generation mechanism in the Loess Plateau, China

Xueli Zhang, Yue Yu, CaiHong Hu and Jianhua Ping

ABSTRACT

In recent years, the amount of water and sediment in the Yellow River Basin has dropped drastically. This paper selected 125 rainfall and flood data points from 1965 to 2015, combined hydrological methods and mathematical statistics to analyze the hydrological factors and runoff generation mechanism, and combined the underlying surface conditions of the Gushanchuan Basin. The characteristics of change revealed the temporal and spatial variation characteristics and related factors of the runoff generation mechanism in the basin. The results showed that the Gushanchuan Basin is still dominated by HOF runoff, but the runoff generation mechanism has also changed with changes in the underlying surface, which are reflected in increased runoff components, the reduced proportion of HOF runoff, and the increased proportion of saturation-excess overland flow (SOF) runoff and mixed runoff. We analyzed the variation law of underlying surface in the basin, which indicated that the increase in the forest grass area was the main factor affecting changes in the watershed runoff generation mechanism. This research will enable a deeper understanding of the runoff generation mechanism of the main soil erosion areas in the Loess Plateau, and reveal variations in the runoff generation mechanism in the Yellow River.

Key words | ecological restoration, Gushanchuan Basin, runoff generation mechanism, vegetation change

Xueli Zhang
CaiHong Hu
Jianhua Ping (corresponding author)
School of Water Conservancy Engineering,
Zhengzhou University,
Science Road 100, Zhengzhou,
China
E-mail: *hkywangjiayi@163.com*

Xueli Zhang
CaiHong Hu
Yellow River Institute for Ecological Protection & Regional Coordinated Development,
Science Road 100, Zhengzhou,
China

Yue Yu
China Machinery International Engineering Design & Research Institute CO., Ltd,
Shaoshan Road, Changsha,
China.

HIGHLIGHTS

- The increase in the forest grass area was the main factor affecting changes in the watershed runoff generation mechanism in Gushanchuan Basin.
- Gushanchuan Basin is still dominated by HOF runoff, and the increased proportion of SOF runoff and mixed runoff.

INTRODUCTION

With continued population expansion, the scale of the economy is expanding, and humans are overly interfering with the natural ecosystems. This interference has resulted in a series of ecological and environmental problems in the Loess Plateau, which is located in the arid and semi-arid regions of the northwest, and has a prominent soil erosion problem (Fu *et al.* 2011). For a long time, water shortages and soil erosion have been sources of restriction of economic development in the Loess Plateau. The area is known as having 'frequent drought and hardship rank first among the world,' and one-fifth of the country's impoverished counties are located in the Loess Plateau (Shi & Shao 2000). Vegetation is an important part of soil and water conservation, it is a core aspect of ecological environmental construction in the Loess Plateau, and it is also one of the primary ways to reverse the ecological environment

doi: 10.2166/ws.2020.361

of the Loess Plateau (Wang *et al.* 2012; Zhao *et al.* 2013). In the past 50 years, this country has successively implemented a series of ecological construction projects, such as key construction of soil and water conservation, construction of the Three-North Shelterbelt System, protection of natural forest resources, returning farmland to forests and grasslands, and construction of silt dams in the Loess Plateau. Most of these major initiatives are based on vegetation restoration and reconstruction, to promote the benign development of the regional water cycle as well as the balance of the socio-economic-ecological complex system. The improvement of soil erosion in the Loess Plateau through vegetation restoration has two aspects: (1) changing the water circulation path to prevent soil erosion, as perennial vegetation can reduce surface runoff by increasing effective vegetation coverage; and (2) increasing soil water content and increasing vegetation productivity (Wang *et al.* 2011).

The Loess Plateau is the main runoff area of the Yellow River Basin. After the 1980s, the Yellow River water volume showed a notable downward trend (Mu *et al.* 2012; Wang *et al.* 2015a, 2015b). The cause of this sharp decline in the Yellow River water volume has been a significant focus of academic debate. Guzha *et al.* (2015) found that land-use change may lead to important changes in runoff generation processes and water storage. Feng *et al.* (2016) pointed out that large-scale vegetation restoration on the Loess Plateau was the main reason for the reduction of water volume in the Yellow River; Miao *et al.* (2012) believed that vegetation restoration on the Loess Plateau made a greater contribution to the reduction of runoff than climate change. Shi *et al.* (2013), however, found that the contribution rate of climate change to the reduction of runoff in the middle reaches of the Yellow River accounted for more than 50%. The impact of land-use change on runoff remains controversial. Currently, most of this research focuses on a quantitative analysis of land-use change on the basin's hydrological cycle. This study explored the reasons for the reduction of water in the Yellow River from the perspective of the runoff generation mechanism. Runoff generation is the process of generating various runoff components in the basin. It is essentially the movement development process of water under the combined effects of various factors affecting the underlying surface and includes the redistribution process of rainfall on the underlying surface (ground and aeration zone). Different underlying surface conditions have different runoff generation mechanisms, and different runoff generation mechanisms affect the development of the entire runoff process, presenting different runoff characteristics (Lee & Huang 2013).

The runoff generation mechanism has three types of characteristics: (1) infiltration-excess (Hortonian) overland flow (HOF), (2) saturation-excess overland flow (SOF), and (3) a combination of HOF and SOF (mixed runoff). HOF is generated when the precipitation rate exceeds the infiltration capacity of the soil or land surface. This can be a dominant process in urbanized or otherwise disturbed areas as well as in areas that typically receive high-intensity precipitation and have a low permeable crust at the soil surface (Horton 1933). SOF is generated when the soil becomes saturated to the extent that additional precipitation cannot infiltrate. Saturation-prone areas include those with a high water table and shallow soils that provide little additional storage for water (Dunne & Black 1970a). The Loess Plateau is characterized by sparse rainfall, high rainfall intensity, and low vegetation coverage, and the thickness of the aerated zone reaches tens of or even hundreds of meters, which is typical of an HOF area (Jiao *et al.* 2017).

This study identified the Gushanchuan Basin in the middle reaches of the Yellow River as the study area. On the basis of an analysis of the underlying surface changes in the Gushanchuan Basin, we distinguished the runoff mechanism of the floods in the basin according to long-term sequence rainfall runoff data and flood data for the Gushanchuan Basin. This study provided insight into the changes in the runoff generation mechanism of the Gushanchuan Basin over the past 40 years, examined reasons for the reduction of the Yellow River water volume from the perspective of the runoff generation mechanism, and provided the necessary scientific basis for the effectiveness of the ecological construction of the Loess Plateau and the formulation of regional sustainable development countermeasures.

MATERIALS AND METHODS

Study area

The Gushanchuan Basin is a primary tributary on the right bank of the middle reaches of the Yellow River in Shaanxi and Inner Mongolia (110°32′24″ – 111°05′24″E,

39°00′00″ – 39°27′36″N), originating from Urigol Township, Junggar Banner, Inner Mongolia, through the Junggar Banner and Fugu County of Shaanxi Province. The basin flows into the Yellow River near Fugu Town, with a drainage area of 1,272 km^2 (above the Gaoshiya Hydrological Station), and has an average annual rainfall of 410 mm. The interannual variation of rainfall is uneven and unevenly distributed; in the flood season (June–September), rainfall can account for 80% of the annual rainfall. As of 2010, the runoff reduction rate in the Gushanchuan Basin was 81%, and the annual average runoff reduction was 1,352,400 m^3/s (Yao *et al.* 2012). In the 1970s, a significant number of soil and water conservation measures were implemented in the Gushanchuan Basin. By 2015, a total of 49 small and medium silt dams were built, with a dam area of 8.90 km^2 and a terrace ratio of 3%. The scale of terraces has increased gradually, and the number of reservoirs has also increased (Wang *et al.* 2015a, 2015b). The four rainfall stations in the basin are the Xinmiao, Xinmin, Gushan, and Gaoshiya stations (Figure 1).

Data collection

This study collected data on annual runoff, daily runoff, sedimentation, and flood data from the Gaoshiya Hydrological Station in Gushanchuan Basin from 1965 to 2015 and collected daily rainfall data from four rainfall stations in the Gushanchuan Basin (Xinmiao, Xinmin, Gushan, and Gaoshiya stations) from 1965 to 2015. We unified data into 1 h time-steps. The runoff data was flood extract data from outlet station (Gaoshiya hydrology station) of Gushanchuan basin from 1965 to 2015. All the above data were obtained from the Yellow River Hydrological Yearbook. The watershed digital elevation model (DEM) had a resolution of 30 m. We derived the land-use data of the Gushanchuan Basin from the Chinese Geospatial Data Cloud with a resolution of 1 km × 1 km.

According to changes in the underlying surface of the Gushanchuan Basin, we divided the research into three stages based on human activities (not considering climate change): the first stage was from 1965 to 1979 and represented the conditions of no human activities; the second stage was from 1980 to 1998 and represented the transition period of human activities on the underlying surface of the basin; the third stage was the severe human activities stage from 1999 to 2015 ('Grain for Green' project was conducted by Chinese government since 1999). We followed the principle that the flood peak flow was greater than 100 m^3/s, the rainfall interval was not more than 24 h, and we unified runoff data into 1 h time-steps. The first stage (1965–1979) included 60 flood events, the second stage (1980–1998) included 50 flood events, and the third stage (1999–2015) included 15 flood events, for a total of 125 flood events to analyze the runoff generation mechanism.

Runoff generation mechanism

Due to the uneven spatial distribution of rainfall and underlying surface conditions, the runoff mechanism is changing during the rainfall process, and nine types of different runoff mechanisms are combined under specific aerated zone structures and rainfall characteristics (Dunne & Black 1970b) (Table 1). However, according to the impact

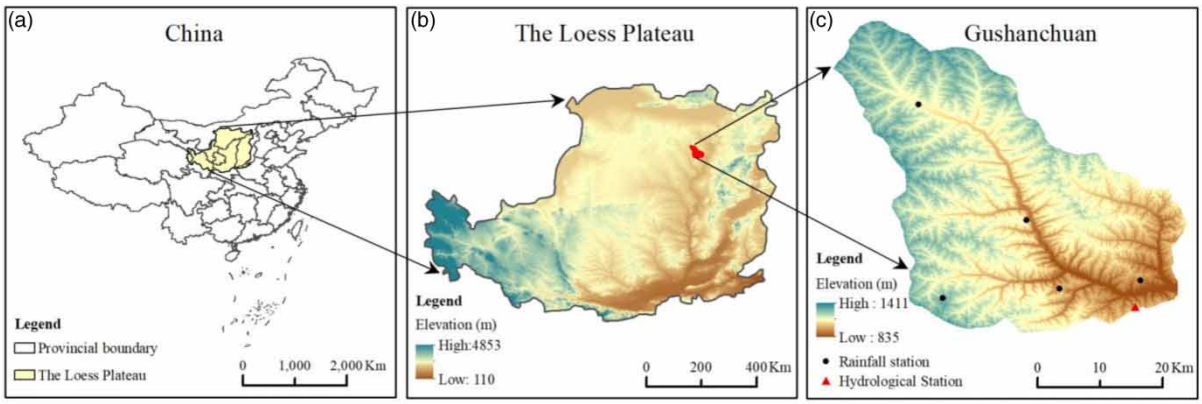

Figure 1 | Relative position of Gushanchuan Basin and distribution map of rainfall stations.

Table 1 | Combination of runoff generation mechanism

Types	Composition of runoff	Impact factors	Types	Composition of runoff	Impact factors
1	$R = R_s$	P, E, W_0, i	6	$R = R_{sat} + R_{int}$	P, E, W_0, i
2	$R = R_s + R_g$	P, E, W_0	7	$R = R_{sat} + R_{int} + R_g$	P, E, W_0
3	$R = R_g$	P, E, W_0	8	$R = R_{int}$	P, E, W_0, i
4	$R = R_s + R_{int}$	P, E, W_0, i	9	$R = R_{int} + R_g$	P, E, W_0
5	$R = R_s + R_{int} + R_g$	P, E, W_0			

factors, it can be divided into two kinds of patterns, namely the infiltration-excess (Hortonian) overland flow (HOF), saturation-excess overland flow (SOF). Generally, the impact factors of SOF are P, E, W_0, and the HOF are P, E, W_0, i (Rui *et al.* 2009), which is expressed as:

$$R = f_{HOF}(P, E, W_0, i) \tag{1}$$

$$R = f_{SOF}(P, E, W_0) \tag{2}$$

where R is runoff depth generated by rainfall (mm); P is the total amount of precipitation (mm); E is watershed evapotranspiration (mm); W_0 is initial water storage capacity (mm); i is rainfall intensity (mm/h).

Because of the spatial and temporal distribution nonuniformity of rainfall and the complexity of the underlying surface, for a specific watershed the runoff generation mechanism is not static and it is difficult to quantify with simple indicators. This study analyzed the composition of watershed runoff components from the flood flow process line (Birtles 1978). According to the principle of runoff generation (Kirkby 1985), the main components of the runoff in the three sections were surface runoff, interflow, and ground runoff. We used Dunne's flow theory (Dunne & Black 1970b) and a flow pattern comprehensive analysis table (Table 2) combining rainfall, rainfall intensity, runoff depth, and pre-influence rainfall to classify the runoff pattern into HOF and SOF from the perspective of quantitative, qualitative, and runoff impact factors. The mixed-flow pattern included both HOF and SOF in a rainfall event, which we comprehensively analyzed and judged.

We used the slope method to separate the baseflow for the flow process line of each rainfall sample. We determined the

Table 2 | Comprehensive analysis table of production flow patterns

Items	Dunne runoff	Horton runoff
Average annual rainfall	>1,000 mm	<400 mm
Average annual runoff coefficient	>0.4	<0.2
Symmetry of flow process line	High	Low
Impacts of rainfall intensity	Low	High
Influencing factors of flow	*API*, rainfall	*API*, rainfall intensity
Surface soil structure	Loose	Compact
Water shortage	Small	Big
Proportion of ground runoff	High	Low
Closeness	Closely related to rainfall	Closely related to rainfall intensity

runoff generation pattern based on the characteristics of rainfall, rainfall density, runoff coefficient, and antecedent precipitation index (*API*). If a flood event had only surface runoff, we defined it as HOF, and if a flood event had ground runoff, considered it to be SOF, other conditions were mixed runoff mechanism. We used flood no. 19770804 as an example to explain the determination process of the runoff generation mechanism (Figure 2) (Hu *et al.* 2020a). No rainfall occurred for 20 days before the flood. In the early stage of the flood, the *API* was very small, the flow process line showed a multipeak type, the main runoff generation mechanism was the surface runoff (R_s), the rate of water retreat was fast, and the flow process line steeply rose and fell. With continuous rainfall, soil water content increased continuously, and the interflow (R_{int}) and groundwater runoff (R_g) were revealed after point B. Because of different confluence speeds, the flood process line presented a steep rise and slow fall in the later stage (Hu *et al.* 2020b). The runoff mechanism was converted from R_s to $R_s + R_{int} + R_g$, and thus this flood had a mixed runoff mechanism.

Rainfall and runoff

We calculated surface rainfall using the Thiessen polygon method. Rainfall duration was an effective duration and did not take intermittent time into account. The ratio of

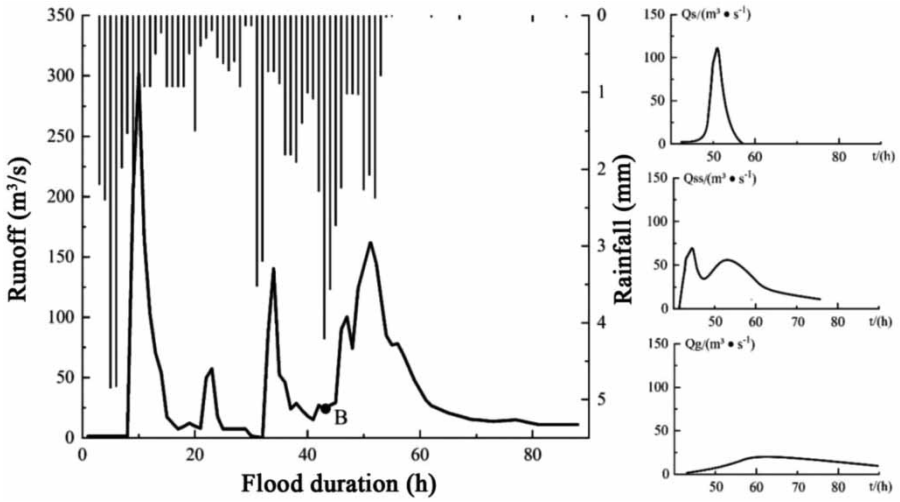

Figure 2 | The schematic diagram of runoff generation discrimination.

surface rainfall-to-rainfall duration was the average rainfall intensity. The rainfall runoff correlation map was a quantitative correlation map established by the average surface rainfall of the floods and the corresponding total runoff and the main factors affecting the relationship between rainfall and runoff (Linsley *et al.* 1975). After using the split flow method to divide the base flow generated by this noncurrent rainfall, we used the storage-discharge relationship method (Ajami *et al.* 2011) to calculate the runoff depth R:

$$R = \frac{3.6\Delta t\left[\sum_{i=2}^{n-1} Q_i + \frac{Q_1 + Q_n}{2} + (Q_n - Q_1)K\right]}{A} \tag{3}$$

where Δt is the period length (h); Q_i is the i-period flow (m^3/s); n is the number of periods; A is the basin area (km^2); and K is the storage coefficient.

Antecedent precipitation index

The antecedent precipitation index (API) reaction was the amount of rainfall that was retained in the soil during the previous rainfall. In this study, we used the recursive formula method (Heggen 2001) to estimate the amount of rainfall affected in the early stage of the flood. According to its definition

$$API_t = kP_{t-1} + k^2P_{t-2} + \ldots + k^n(API_{t-n} + P_{t-n}) \tag{4}$$

From this, the formula for calculating the amount of rainfall in the early stage is derived:

$$P_{a,t+1} = k(P_{a,t} + P_t) \tag{5}$$

where API_t is the previous impact rainfall (mm) on day t; API_{t+1} is the previous impact rainfall (mm) on $t+1$ day; n is the number of previous rain days affecting the runoff, which was usually about 15 days; P_t is the t-day rainfall (mm); P_{t-1}, P_{t-2} … is the rainfall (mm) on 1 day before t day, 2 days before …; and k is the daily decrease coefficient of the soil water content.

Catchment water storage capacity

We derived the catchment water storage capacity (W_m) from successive floods that included multiple floods (Llorens & Gallart 2000). The calculation selected the rainfall floods that saturated the water content of the basin and produced a large flood process. The process is as follows:

Let $W_{m,\ 0} = I_m$, where the loss is $I_m = P - R$, P is the total amount of rainfall, and R is the total amount of runoff depth generated by rainfall (Hu *et al.* 2016). The calculation process of W_m follows:

$$K_j = 1 - \frac{k_e \times E_0}{W_{m,j}} \tag{6}$$

$$W_{0,j} = \sum_{0}^{n} P_i \times K_j^i \tag{7}$$

and

$$W_{m,j} = W_{m,j-1} + W_{0,j-1} \tag{8}$$

where k_e is the evapotranspiration capacity of the basin, the ratio of E_m to water surface evaporation; K_j is the constant coefficient; P_i is the effective rainfall for the i day before the flood; i is the power; j is the number of iterations; and $W_{m,0}$ is the assumed value for the first iteration. After several iterations, W_m tends toward a stable value, which represents the water storage capacity of the basin.

Runoff and meteorology factors, underlying surface conditions

We used principal component analysis (*PCA*) to determine the relationship between the runoff coefficient (α) of a rainfall event and potential evapotranspiration (ET_0), rainfall (P), antecedent precipitation index (API), maximum rainfall density (I_{max}), mean rainfall intensity (I_{mean}), leaf area index (LAI), vegetation coverage (V_c), and rainfall duration (t). We calculated ET_0 according to the Penman-Monteith method, determined P_a by the recursive formula method, and obtained LAI and V_c from remote-sensing data by ENVI 5.0. Then, we used the theory of multiple nonlinear regression analysis to determine the relationship between the runoff coefficient of the rainfall event and the principal components.

Curve estimation model

Curve estimation theory could use one variable to predict another variable. The mathematical models are presented in Table 3. When an optimal model cannot be determined based on observations immediately, a simple and more suitable model can be established from many regression models using the curve estimation method. Curve estimation requires that the independent and dependent variables belong to numeric variables.

Goodness-of-fit test

We used the determination coefficient (R^2) as the criterion for a goodness-of-fit test to select the following curve equation:

Table 3 | Form of curve estimation model

Model name	Model expression
Linear function of one variable	$Y = b_0 + b_1 x$
Quadratic function	$Y = b_0 + b_1 x + b_2 \times^2$
Composite function	$Y = b_0 (b_1)^x$
Growth function	$Y = e^{(b_0 + b_1 x)}$
Logarithmic function	$Y = b_0 + b_1 \ln x$
Cubic function	$Y = b_0 + b_1 x + b_2 \times^2 + b_3 \times^3$
S curve	$Y = e^{(b_0 + b_1/x)}$
Exponential function	$Y = b_0 e^{b_1 x}$
Inverse function	$Y = b_0 + b_1/x$
Power function	$Y = b_0 x^{b_1}$
Logic function	$Y = (1/u + b_0 b_1 x)^{-1}$

$$R^2 = \frac{SSR}{SST} = 1 - \frac{SSE}{SST} = 1 - \frac{\sum (y - \hat{y})^2}{\sum (y - \bar{y})^2} \tag{9}$$

where SSR is the regression sum of squares; SSE is the sum of squares of residuals; and SST is the sum of total deviations squared. The determination coefficient is a comprehensive measure of the goodness of fit of the regression model. The larger the evaluation coefficient, the higher the model's goodness of fit.

Significance test of the regression equation

We used an F-test to test the significance of the established regression equation. The F-test is the ratio between the average regression sum of squares and the average residual sum of squares:

$$F = \frac{SSR/k}{SSE/(n-k-1)} = \frac{\sum (\hat{y} - \bar{y})^2 / k}{\sum (\hat{y} - \bar{y})^2 / (n-k-1)} \tag{10}$$

where n is the sample numbers; and k is the number of independent variables.

Data analysis

We statistically analyzed rainfall characteristics, runoff, and sedimentation. We evaluated data using SPSS for Windows

16.0 (SPSS Inc., Chicago, IL, USA). We used one-way analysis of variance (ANOVA) to assess the influence of runoff for sedimentation and the relationship between runoff and rainfall, and rainfall density.

RESULTS AND DISCUSSION

Characteristics of rainfall and flood

As time has passed, the annual runoff and sedimentation have shown a decreasing trend in Gushanchuan Basin. The peak runoff corresponded to the peak sedimentation. By 2015, the runoff reduction rate was 81%, and the annual runoff reduction was 1.35 billion m^3 (Figure 3(a)), and the correlation between annual runoff and sediment was significant (Figure 3(b)). The results showed that soil and water conservation has played an obvious role in recent decades, and as a result, soil erosion has decreased sharply.

Because of the influence of rainfall and underlying surface changes, the rainfall-runoff relationship at each stage was different. The three-stage rainfall-runoff correlation coefficients were 0.59, 0.53, and 0.70. In comparison, the third-stage runoff had the strongest dependence on rainfall, and rainfall in the third stage decreased significantly (Figure 4). The correlation coefficients between rainfall intensity and runoff were 0.59, 0.62, and 0.51 for the three stages. For rainfall events of the same magnitude of rainfall intensity in these three stages, the first stage had the largest runoff, and the third stage had the smallest runoff (Figure 4).

The rainfall duration of the Gushanchuan Basin increased first and then decreased, and most of the rainfall lasted between 20 and 40 h. The rainfall at each stage was 69.6, 55.4, and 24.8 mm. We categorized flood generation in four levels: light rain (<10 mm), moderate rain (10–25 mm), heavy rain (25–50 mm), and rainstorm (50 mm). Among the 125 flood events, there were 19 light rains, 42 moderate rains, 36 heavy rains, and 28 rainstorms. Therefore, we determined that the Gushanchuan Basin suffered primarily from moderate rains and heavy rains. The flood duration also showed a first increasing and then a decreasing trend, and the peak flow showed a significant decrease over the year (Table 4).

Analysis of underlying surface changes

The grassland area in the Gushanchuan Basin accounted for the largest proportion of land (61–63%), which was followed by farmland (31–33%). The urban construction land area accounted for the smallest proportion of land (0.35%–0.55%). Between 1976 and 2015, the area of farmland decreased year by year, and the area of forestland, grassland, and urban construction land increased to different extents,

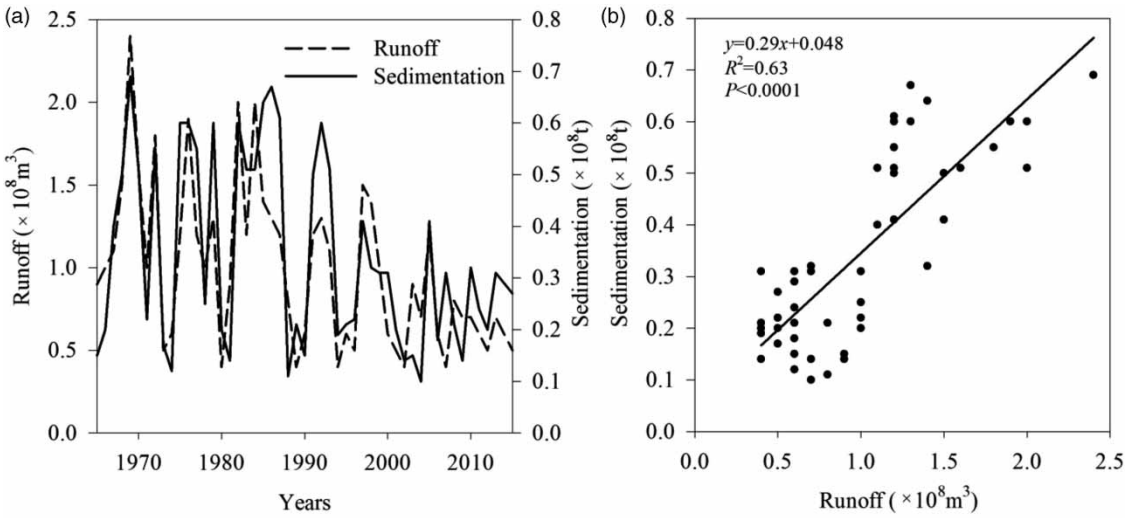

Figure 3 | Annual variation of runoff and sediment from 1965 to 2015.

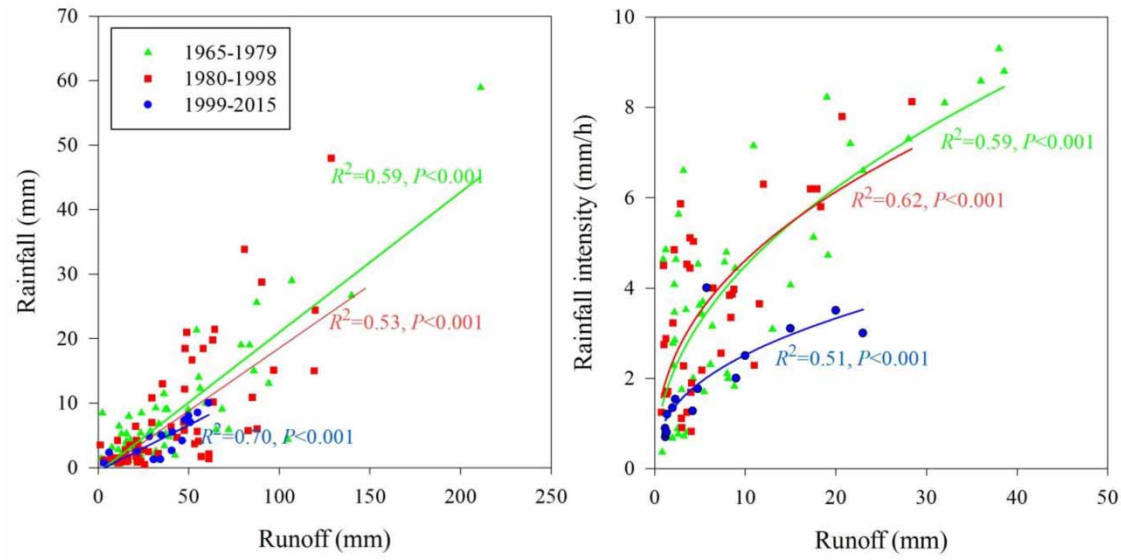

Figure 4 | The relationships between rainfall and runoff in Gushanchuan Basin.

Table 4 | Characteristics of rainfall and flood in different stages of Gushanchuan basin

Item	1965–1979	1980–1998	1999–2015
Mean rainfall duration (h)	40.8	48.9	35.5
Mean rainfall (mm)	69.6	55.4	24.8
Mean flood duration (h)	122.4	143.1	103.4
Mean peak flow (m^3/s)	1,978.6	1,030.5	214.9

but the water area remained basically stable. In addition, farmland showed the greatest change in area among all land-use types. The total cultivated area of 24.52 km^2 was converted to other land-use types. The main forms of land conversion were farmland into forestland and grassland into forestland. The forestland area increased by 18.22 km^2. The area increased by 5.39 km^2, which indicated the significant effect of 'returning farmland to forests' and 'returning farmland to grassland,' and the area of forestland and grassland also increased significantly (Figure 5, Table 5).

Runoff and meteorology factors, underlying surface conditions

We obtained three principal components (P, API, and V_c) based on the PCA. We obtained the expressions between each independent variable and dependent variable according to curve estimation. We took the runoff coefficient (α) as the dependent variable, and rainfall (P), antecedent precipitation index (API), and vegetation coverage (V_c) as independent variables. The expression was as follows:

$$\alpha = \frac{a}{P} + b \cdot API + c \cdot \sin\left(3.14\frac{V_c - d}{e}\right) + f \quad (11)$$

where a, b, c, d, and e are the fitting parameters, and f is the constant. Other parameters have the same meanings as noted earlier. We obtained fitting parameters by nonlinear regression (Tables 6 and 7).

In this study, we combined the curve estimation method with the multivariate nonlinear regression analysis, which we used to build the runoff coefficient prediction model. The main factors affecting runoff coefficient included rainfall (P), antecedent precipitation index (API), and vegetation coverage (V_c). The runoff coefficient prediction model had high precision and a certain theoretical significance and research value, which provided additional references for the runoff simulation (Figure 6).

The runoff generation mechanism

From 1965 to 2015, the Gushanchuan Basin was dominated by HOF, accounting for 62.4% of the flood events. Mixed

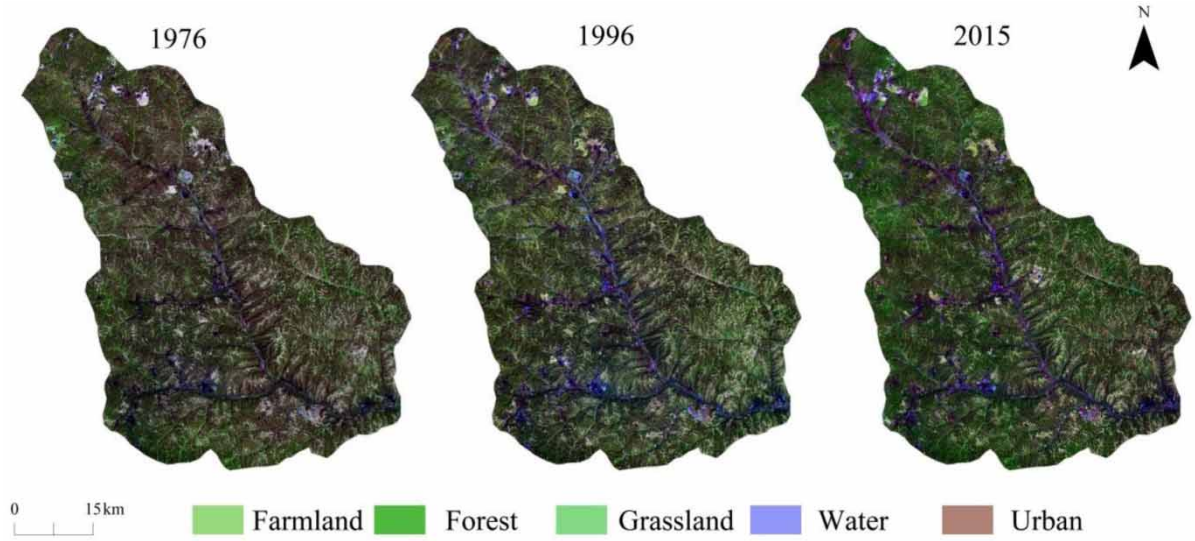

Figure 5 | Land-use change map of Gushanchuan Basin.

Table 5 | Land use classification statistics

	Type					
Year	Farmland/km²	Forest/km²	Grass/km²	Water/km²	Urban construction/km²	Sum/km²
1976	413.68	65.47	774.55	12.28	6.02	1,272
1996	405.94	78.41	800.32	12.82	4.51	1,272
2015	389.16	89.69	779.94	12.16	7.05	1,272
Average	402.93	69.91	784.94	12.42	5.86	1,272
Proportion, %	31.68	5.18	61.71	0.97	0.46	100

Table 6 | Estimation results of nonlinear regression parameters

			95% confidence interval	
Parameters	Values	Standard error	Lower limit	Ceiling
a	0.799	0.796	0.407	1.192
b	0.008	0.001	0.005	0.011
c	−0.015	0.008	−0.031	0.001
d	0.106	0.013	0.080	0.132
e	0.013	0.000	0.012	0.013
f	0.037	0.011	0.016	0.059

Table 7 | Variance analysis table

Source	Sum of squares	Degrees of freedom	Mean square
Regression	1.07	6	0.18
Residual	0.12	56	0.002
Before revision	1.19	62	
After revision	0.41	61	

Dependent variable: runoff coefficient; $R^2 = 1$-(Sum of squares of residuals)/(Corrected sum of squares) = 0.709.

runoff accounted for 35.2% of the flood events, and SOF accounted for only three flood events. The flood events with HOF as the main pattern accounted for 72, 58, and 40% for 1965–1979, 1980–1998, and 1999–2015, respectively. The proportion of HOF events decreased significantly from 1965 to 2015. The proportion of flood events with mixed runoff as the main mode of runoff in each of the three stages was 28, 40, and 47%. In general, the HOF was dominant in each stage but the proportion of events decreased, whereas SOF and mixed runoff increased (Table 8).

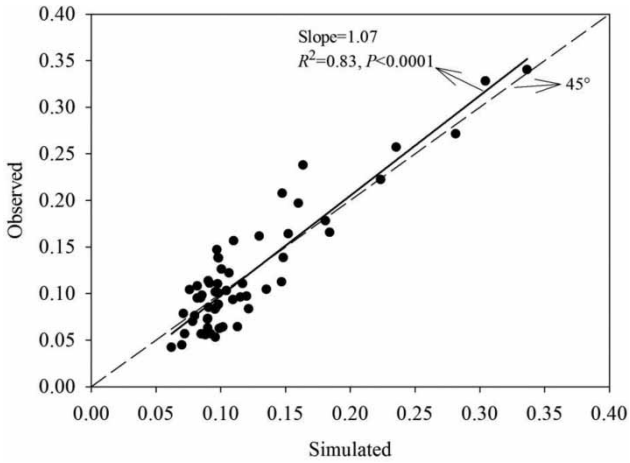

Figure 6 | The relationships between observed and simulated values of runoff coefficient.

Table 8 | Statistics on flood generation and flow patterns in different stages

	Pattern			
Year	Horton runoff	Dunne runoff	Mixed runoff	Sum
The first stage 1965–1979	43 (72%)	0 (0%)	17 (28%)	60 (100%)
The second stage 1980–1999	29 (58%)	1 (2%)	20 (40%)	50 (100%)
The third stage 2000–2015	6 (40%)	2 (13%)	7 (47%)	15 (100%)
Sum	78 (63%)	3 (2%)	44 (35%)	125 (100%)

The effect of land-use cover changes on runoff

Groundwater outflow

In the Gushanchuan Basin, forest area increased rapidly. Previous studies found that discharge capacity had an influence on underground water and minimum daily discharge in the flood season (Bronstert *et al.* 2002; Doerra *et al.* 2006). Annual mean minimum daily flow and the minimum daily flow in the flood season showed obvious increasing trends from 1965 to 2015, and it was easier to generate underground flow and interflow (Table 9) (Walker *et al.* 1993; Loch 2000). As confluence time expanded, the flood process changed: forest areas increased 73%, which resulted in an 87% increase in groundwater outflow (Table 9).

Table 9 | Statistics on the convergence characteristics of Gushanchuan Basin

Items	1965–1978	1979–1998	1999–2015
Forest areas (km²)	65.47	78.41	89.69
Annual average minimum flow (m³/s)	0.68	1.26	1.40
Minimum daily flow in the flood season (m³/s)	1.93	2.61	3.30
Averaged rainfall before generate flow(mm)	6.9	9.4	21.0
Duration of flood subsidence (h)	14.22	14.39	16.38
Catchment water storage capacity (mm)	101.37	124.73	156.36

Infiltration capacity

The forest areas increased by 27%, rainfall required before runoff generation increased by 192%, and the duration of flood subsidence increased by 22% (Table 9). This is because increasing forest area will increase rainfall interception and soil infiltration capacity. In the early stage of a storm, rainfall is consumed by the infiltration. Flood subsidence is an important aspect of runoff generation and confluence. A certain amount of infiltration occurs during the process of flood subsidence. Generally speaking, with an increase in rainfall and rainfall intensity, the runoff coefficient will also increase. As the years passed, more rainfall was needed in the Gushanchuan Basin to produce runoff, which indicated that infiltration had increased gradually. The duration of flood subsidence also increased gradually (Table 9). Averaged rainfall before generated flow and catchment water storage capacity increased from 1965 to 2015, which indicated an increase in infiltration, resulting in an increase in soil moisture. Equations (1) and (2) illustrated that the runoff generation was related to soil moisture, thus this increase in infiltration is an important reason for changes in runoff generation and for the confluence mechanism of the basin. The increase in soil moisture enhancement resulted in a decrease in surface runoff, runoff coefficient, and flood peak flow, and in an increase in underground runoff and confluence duration (Merz & Blöschl 2009). Our previous study also found that flood events with SOF increased as flood events with HOF decreased because of increased forest areas (Li 2018).

Forest and grasslands had greater steady infiltration rates than farmland (Archer *et al.* 2002; Jian *et al.* 2012). Vegetation influenced the chemistry, structure, organic content, and strength of the soil. Roots and burrowing organisms bioturbated the soil, changed the pathways, and generally increased porosity and infiltration capacity (Gabet *et al.* 2003; Thompson *et al.* 2010). As a consequence, alterations in vegetation may create broad-scale changes in the way rainfall is partitioned into runoff and recharge. Infiltration capacity is a commonly used term to reflect the maximum rate at which soils can absorb water, which generally occurs under dry conditions when supportive influences are greatest. The infiltration capacity tended to decrease as the soil moisture content of the surface layers increased (Jian *et al.* 2014). In general, more deeply rooted species can change soil properties to suit their water-use needs (Hirota *et al.* 2004). Spatial variations in hydrology and soil characteristics are not represented in this analysis, and those differences likely are the reason for the large site-to-site differences. For example, bare soil in one location may have a higher infiltration than grasses at another location, which likely can be attributed to other soil-forming factors, such as parent material, topography, aspect, climate, and soil age. This study, however, did show promise for the generalization of local or perhaps even island-wide trends, which allows for mappable units of infiltration properties that could be related to processes of interest, including areas of potentially high-aquifer recharge or erosion susceptibility.

Water storage capacity

The water storage capacity of the Gushanchuan Basin increased year by year (Table 9). Previous studies have shown that the water storage capacity of woodland was higher than other land-use covers and that an increase in forest areas would result in the increase of catchment water storage capacity and reducing runoff (Jian *et al.* 2016). The forest areas increased by 37% as the water storage capacity increased by 54% (Table 9); other studies have found similar results (Mascha *et al.* 2009). In Gushanchuan Basin, both SOF and HOF were evident. Our previous study found that the flood events were mainly HOF, and the SOF flood events showed an increasing trend in Gushanchuan Basin (Li 2018).

CONCLUSIONS

The effect of forest vegetation coverage on runoff generation mechanism is very significant in the Gushanchuan basin. This information enabled us to more deeply understand the water production law of the main soil erosion areas in the Yellow River Basin and revealed the mechanism of water quantity change in the Yellow River. The outcomes are of great significance for the local government to carry out vegetation restoration, a preliminary understanding is as follows: (1) it is necessary to fully understand the ecological benefits of forest vegetation in conserving water resources and reducing flood peak flow, establish long-term water resources strategic; (2) It is necessary to return cultivated land to forests, establish a complex system of agriculture, forest and water, and realize a virtuous cycle of ecological environment in the basin; (3) it would establish an industrial structure that combines agriculture with forestry to achieve sustainable economic development.

Land-use change is an important factor that cannot be ignored in causing runoff changes, particularly in the flood season. Because of the impact of land-use change on water resources and ecosystem health in the Gushanchuan Basin, appropriate consideration should be given to the role played by land-use change. In fact, climate change should be considered when assessing the impact of future land-use cover changes. The combined effects of climate and land-use cover changes are complex, however, and are beyond the scope of this paper. Future research will consider land-use prediction models based on cellular automaton and Markov chains and will be combined with regional future climate scenarios to quantitatively predict future land-use and climate change impacts on runoff.

ACKNOWLEDGEMENTS

This project was supported by the National Key Research Priorities Program of China (2016YFC0402402); National Natural Science Foundation of China (31700370); The

open fund of Key Laboratory of Yellow River sediment of the Ministry of Water Resources; National Natural Science Foundation of China (51409116); Startup Research Fund of Zhengzhou University (1512323001); Institution of higher learning key scientific research project, Henan Province (16A570010); Foundation of Drought Climate Science (IAM201705); China Postdoctoral Science Foundation (2016M602255); Henan Province Postdoctoral Science Foundation; National Natural Science Foundation of China (91025015). We would like to thank LetPub (www.letpub.com) for providing linguistic assistance during the preparation of this manuscript.

CONFLICT OF INTEREST

The authors declared that they have no conflicts of interest to this work. We declare that we do not have any commercial or associative interest that represents a conflict of interest in connection with the work submitted.

DATA AVAILABILITY STATEMENT

All relevant data are available from an online repository or repositories at http://www.yrcc.gov.cn/.

REFERENCES

Ajami, H., Troch, P. A., Maddock III., T., Meixner, T. & Eastoe, C. 2011 Quantifying mountain block recharge by means of catchment-scale storage-discharge relationships. *Water Resources Research* **47** (4), W04504.

Archer, N., Quinton, J. N. & Hess, T. M. 2002 Below-ground relationships of soil texture, roots and hydraulic conductivity in two-phase mosaic vegetation in South-east Spain. *Journal of Arid Environments* **52** (4), 535–553.

Birtles, A. B. 1978 Identification and separation of major base flow components from a stream hydrograph. *Water Resources Research* **14** (5), 791–803.

Bronstert, A., Niehoff, D. & Burger, G. 2002 Effects of climate and land-use change on storm runoff generation: present knowledge and modelling capabilities. *Hydrological Processes* **16** (2), 509–529.

Doerra, S. H., Shakesbya, R. A., Blakeb, W. H. & Chaferc, C. J. 2006 Effects of differing wildfire severities on soil wettability and implications for hydrological response. *Journal of Hydrology* **319**, 295–311.

Dunne, T. & Black, R. D. 1970a An experimental investigation of runoff production in permeable soils. *Water Resources Research* **6** (2), 478–490.

Dunne, T. & Black, R. D. 1970b Partial area contributions to storm runoff in a small New England watershed. *Water Resources Research* **6** (5), 1296–1311.

Feng, X. M., Fu, B. J., Piao, S. L., Wang, S., Ciais, P., Zeng, Z. Z., Lu, Y. H., Zeng, Y., Li, Y., Jiang, X. H. & Wu, B. F. 2016 Revegetation in China's loess plateau is approaching sustainable water resource limits. *Nature Climate Change* **6** (111), 1019.

Fu, B. J., Liu, Y., Lu, Y. H., He, C. S., Zeng, Y. & Wu, B. F. 2011 Assessing the soil erosion control service of ecosystems change in the Loess Plateau of China. *Ecological Complexity* **8** (4), 284–293.

Gabet, E. J., Reichman, O. J. & Seabloom, E. W. 2003 The effects of bioturbation on soil processes and sediment transport. *Annual Review of Earth and Planetary Sciences* **31** (1), 249–273.

Guzha, A. C., Nobrega, R. L., Kovacs, K., Rebola-Lichtenberg, J., Amorim, R. S. S. & Gerold, G. 2015 Characterizing rainfall-runoff signatures from micro-catchments with contrasting land cover characteristics in southern Amazonia. *Hydrological Processes* **29** (4), 508–521.

Heggen, R. J. 2001 Normalized antecedent precipitation index. *Journal of Hydrologic Engineering* **6** (5), 377–381.

Hirota, I., Sakuratani, T., Sato, I., Higuchi, H. & Nawata, E. 2004 A split-root apparatus for examining the effects of hydraulic lift by trees on the water status of neighbouring crops. *Agroforestry Systems* **60** (2), 181–187.

Horton, R. E. 1933 The role of infiltration in the hydrologic cycle. *Transactions, American Geophysical Union* **14** (1), 446.

Hu, C., Li, S., Zhang, W., Chen, X. & Wang, J. 2016 Establishing and testing runoff model based on runoff coefficient. *Journal of China Hydrology* **36**, 8–13 (in Chinese with English abstract).

Hu, C. H., Ran, G. & Jian, S. Q. 2020a Effect of forest and grass cover change on runoff mechanism in Jialu River Basin. *Journal of Soil and Water Conservation* **34** (2), 36–42 (in Chinese with English abstract).

Hu, C. H., Zhang, L., Wu, Q., Soomro, S. & Jian, S. Q. 2020b Response of LUCC on runoff generation process in middle Yellow River Basin: The Gushanchuan Basin. *Water* **12**, 1237.

Jian, S. Q., Zhao, C. Y., Fang, S. M., Yu, K. & Peng, S. Z. 2012 Characteristics of rainfall interception by *Caragana korshinskii* and *Hippophae rhamnoides* in Loess Plateau of Northwest China. *The Journal of Applied Ecology* **23** (9), 2383–2389 (in Chinese with English abstract).

Jian, S. Q., Zhao, C. Y., Fang, S. M. & Yu, K. 2014 Soil water content and water balance simulation of *Caragana korshinskii* Kom. in the semiarid Chinese Loess Plateau. *Journal of Hydrology and Hydromechanics* **62** (2), 89–96.

Jian, S. Q., Zhang, X. L., Wu, Z. N. & Hu, C. H. 2016 Water use pattern of *Pinus tabulaeformis* in the semiarid region of loess plateau, China. *Forest Systems* **25** (3), 77.

Jiao, Y., Lei, H., Yang, D., Huang, M., Liu, D. & Yuan, X. 2017 Impact of vegetation dynamics on hydrological processes in a semi-arid basin by using a land surface-hydrology coupled model. *Journal of Hydrology* **551**, 116–131.

Kirkby, M. J., 1985 *Hillslope Hydrology. Hydrological Forecasting*, John Wiley and Sons, New York, NY, 37–75.

Lee, K. & Huang, J. 2013 Runoff simulation considering time-varying partial contributing area based on current precipitation index. *Journal of Hydrology* **486**, 443–454.

Li, N. 2018 *Study on the Mechanism of Runoff Production and Confluence in the Loess Plateau Under the Change of Underlying Surface*. Zhengzhou University, Zhengzhou, China (in Chinese with English abstract).

Linsley Jr., R. K., Kohler, M. A. & Paulhus, J. L. 1975 *Hydrology for Engineers*. McGraw-Hill, New York, NY.

Llorens, P. & Gallart, F. 2000 A simplified method for forest water storage capacity measurement. *Journal of Hydrology* **240** (1), 131–144.

Loch, R. J. 2000 Effects of vegetation cover on runoff and erosion under simulated rain and overland flow on a rehabilitated site on the Meandu mine, Tarong, Queensland. *Australian Journal of Soil Research* **38** (38), 299–312.

Mascha, J., Nadine, W., Christian, P., Matthias, S., Christoph, L., Frank, M. & Thomas, F. M. 2009 Nutrient release from decomposing leaf litter of temperate deciduous forest trees along a gradient of increasing tree species diversity. *Soil Biology & Biochemistry* **41** (10), 2122–2130.

Merz, R. & Blöschl, G. 2009 A regional analysis of event runoff coefficients with respect to climate and catchment characteristics in Austria. *Water Resources Research* **45**, 1.

Miao, C., Shi, W., Chen, X. & Li, Y. 2012 Spatio-temporal variability of streamflow in the Yellow River: possible causes and implications. *Hydrological Sciences Journal* **57** (7), 1355–1367.

Mu, X. M., Zhang, X. Q., Shao, H. B., Gao, P., Wang, F., Jiao, J. Y. & Zhu, J. L. 2012 Dynamic changes of sediment discharge and the influencing factors in the Yellow River, China, for the recent 90 years. *Clean-Soil Air Water* **40** (3), 303–309.

Rui, X., Gong, X. & Zhang, C. 2009 Formation and calculation of watershed runoff yield. *Journal of Hydroelectric Engineering* **28**, 146–156.

Shi, H. & Shao, M. 2000 Soil and water loss from the Loess Plateau in China. *Journal of Arid Environments* **45** (1), 9–20.

Shi, C., Zhou, Y., Fan, X. & Shao, W. 2013 A study on the annual runoff change and its relationship with water and soil conservation practices and climate change in the middle Yellow River basin. *Catena* **100**, 31–41.

Thompson, S. E., Harman, C. J., Heine, P. & Katul, G. G. 2010 Vegetation-infiltration relationships across climatic and soil type gradients. *Journal of Geophysical Research: Biogeosciences* **115**, 1–12.

Walker, J., Bullen, F. & Williams, B. G. 1993 Ecohydrological changes in the Murray-Darling Basin. I. the number of trees cleared over two centuries. *Journal of Applied Ecology* **30** (2), 265–273.

Wang, Y. Q., Shao, M. A., Zhu, Y. J. & Liu, Z. P. 2011 Impacts of land use and plant characteristics on dried soil layers in different climatic regions on the Loess Plateau of China. *Agricultural and Forest Meteorology* **151**, 437–448.

Wang, S., Fu, B. J., Gao, G. Y., Yao, X. L. & Zhou, J. 2012 Soil moisture and evapotranspiration of different land cover types in the Loess Plateau, China. *Hydrology and Earth System Sciences* **16** (8), 2883–2892.

Wang, K., Xia, Y., Ma, J. & Qu, C. 2015a Quantitative Assessment of soil erosion in Gushanchuan watershed based on CSLE and high-resolution aerial images. *Research of Soil and Water Conservation*, 1, 6 (in Chinese with English abstract).

Wang, S., Fu, B. J., Piao, S. L., Lü, Y. H., Ciais, P., Feng, X. M. & Wang, Y. F. 2015b Reduced sediment transport in the Yellow River due to anthropogenic changes. *Nature Geoscience* **9** (1), 38.

Yao, Z. H., Yang, Q. K., Xie, H. X. & Li, R. 2012 Application of Chinese soil loss equation (CSLE) to analyze the spatial and temporal variations in soil erosion on the loess plateau of China. *Journal of Food Agriculture and Environment* **10** (3), 1285–1293.

Zhao, G., Mu, X., Wen, Z., Wang, F. & Gao, P. 2013 Soil erosion, conservation, and eco-environment changes in the loess plateau of China. *Land Degradation & Development* **24** (5), 499–510.

First received 11 August 2020; accepted in revised form 30 November 2020. Available online 10 December 2020